Proceedings of the Indian National Science Academy (2023) 89:977–987
https://doi.org/10.1007/s43538-023-00212-7

RESEARCH PAPER

Application of response surface-based finite element model in structural damage identification of concrete beams

Peng Weng[1] · Hongyu Hui[2] · Yang Zou[3]

Received: 25 July 2023 / Accepted: 17 September 2023 / Published online: 12 October 2023

Abstract

The emergence of finite element model modification techniques has made it possible to use numerical theoretical analysis techniques to achieve the assessment of the bearing capacity of two problems in practical engineering. Therefore, an improved scheme of finite element model based on the response surface method is proposed, which is optimized by GA algorithm and verified. The experimental results show that the mid-span deformation and strain of the beam under static load are below 5%. Under different static responses, the deformation amplitude is within the set range of concrete structure failure, and has high sensitivity. The precision of response surface equation under different static responses is above 0.99, the highest is 0.9996, which shows the good fitting accuracy of the model. The calculated results of the two optimal methods are in good agreement with the measured results, and the deviation comparison values are within 10%, the lowest is 1.1%. It can identify the concentrated parts of the concrete beam, which is basically consistent with the actual results. In summary, the improved finite element model of response surface can be used to better judge the stress status of concrete beams. Through optimization such as genetic algorithms, the damage identification rate of structures can be effectively improved, which is of great significance in practical engineering applications.

Keywords Response surface · Finite element model · Concrete beam · Structural damage identification

Introduction

Rapid economic development has promoted road traffic construction to meet the rapid development. As an important transportation hub for crossing obstacles and connecting different places, bridges play a significant role in highway transportation (Song et al. 2022). With the increase of service time, the existing prestressed concrete beam bridges inevitably have problems such as damage accumulation, so it is necessary to identify and evaluate the bearing capacity of existing bridges (Ma et al. 2022). For this problem, Skokandić & Mandić Ivanković (2022) put forward the technical method of traffic counter and dynamic weighing in the face of the aging problem of highway bridge strips at present. Jawdhari et al. (2022) proposed a stress calculation and analysis method of the reinforced concrete arch culvert for atypical structures. Cui et al. (2022) proposed a complete transfer learning technology for the state evaluation of bridge elastic bearings. Under this background, the finite element model is improved on the basis of response surface. The GA algorithm is used to optimize the modified model to improve the damage identification accuracy of the concrete beam structure, so as to effectively evaluate the bearing capacity of the existing bridge.

✉ Peng Weng
pengwengwp@outlook.com

1 Department of Architecture and Environmental Engineering, Changzhou University Huaide College, Jingjiang 214500, China

2 Rail Transit and Tunnel Design and Research Institute, China Railway Liuyuan Group Co., Ltd, Wuxi 214000, China

3 Second Engineering Company, Shanghai Construction NO.2 (Group) Co., Ltd, Shanghai 200030, China

Literature review

Due to more damage to the bridge structure at present, its bearing capacity and use are increasingly valued, so accurate and effective analysis and evaluation of existing bridges are required to ensure their safety (Wei et al. 2022). The finite element model is modified because the theoretical model in the finite element software is modified by the static and dynamic load test data, which makes the obtained bridge structure response data closer to the measured data (Li e al. 2020). Therefore, the majority of domestic and foreign scholars have conducted in-depth research on it. Wu & Liu (2022) optimized the modification method of the parametric finite element model for the health monitoring of long-span bridges, so as to effectively improve the accuracy of their monitoring. In order to realize the modeling of bridge load under a dynamic state, De Risi (2022) proposed a method of moving load based on the finite element modeling calculation framework, which improved the accuracy of bridge load prediction under a dynamic state. Svendsen et al. (2022) proposed a new program on the basis of updating the finite element model for the problem of bridge life extension, thus providing an effective reference for improving its life. Tran-Ngoc et al. (2022) modified the finite element model of the double steel truss bridge structure monitoring problem by using the vibration measurement and hybrid element heuristic search algorithm to effectively ensure the health of the bridge structure. In order to predict the prestress of cable-stayed bridge cables and the elevation of the bridge deck, Souza Hoffman I et al. conducted a numerical model by using the finite element method, thus providing help for their analysis and prediction (Souza Hoffman et al. 2022). Zaghian et al. (2022) put forward a comprehensive analysis method of corrosion damage in view of the corrosion of bridge concrete reinforcement, so as to effectively reduce the deterioration factors caused by corrosion. Lin et al. (2022) modified the finite element model of small-span concrete culvert bridges by using neural networks to reduce the uncertainty after construction.

In addition, Yu et al. (2022) modified the finite element model by combining a large number of samples to address the seismic problem of trains traveling on bridges, thereby improving the applicability of bridge seismic verification while reducing the distortion of seismic response results. Zhang and Sun (2021) proposed a new method for integrating pattern recognition and finite element model correction by utilizing physically guided machine learning to address related issues in structural health monitoring. This not only improves the universality of structural damage detection, but also improves the performance of bridge structural damage identification. The researchers proposed a new correction method for defects in aluminum alloy structures by conducting detailed analysis of finite element analysis methods, which effectively optimized the defects in aluminum alloy structures. Naranjo-Pérez et al. (2021) proposed a hybrid unscented Kalman filter algorithm to address the related issues of finite element models when dealing with complex structural problems, which effectively improves the performance of effective finite element models. Zhu et al. (2022) built and revised the finite element model for the structural monitoring of steel–concrete composite girder bridges, so as to provide guidance for their safety evaluation. Deng et al. (2022) modified the two-dimensional symmetric finite element model by using an artificial intelligence algorithm to solve the problems related to pavement materials and structures, which provided a reference for solving the problems related to pavement application materials and structures.

From the research of domestic and foreign scholars, the finite element model modification can effectively evaluate the operation safety and damage development of bridges. Therefore, on the basis of previous studies, the response surface method was proposed to modify the finite element model. In order to solve the defects of the response surface method in finding structural parameters, a genetic algorithm (GA) was creatively introduced to achieve optimization. In the research, the theoretical data and the measured data are organically combined, thus making a certain contribution to promoting the safety performance evaluation method of beam structures.

Analysis of response surface model modification in structural damage identification of concrete beams

Finite element model construction and response surface method analysis

To obtain the load-carrying capacity of the actual concrete beam structure and to identify the damage to the structure, the study modified the finite element model by using the response surface method so that the modified finite element model can effectively assess the force and safety state of the actual concrete beam mechanism and was verified in the actual damage identification. A finite element model is established by the finite element method, which is a set of assemblies that are connected and transfer forces only by the nodes, and are constrained only at the nodes (Manoj et al. 2022). In computer applications, finite element analysis software (ANSYS) is a widely used large-scale finite element software, which plays a pivotal role in the design and use of bridge structures (Wang et al. 2022). A finite element model is established, which is an approximate simulation of a solid beam-type structure in the field so that it has theoretical components that meet the engineering accuracy requirements and gives boundary conditions that approximate the actual ones and thus simulate them. The software has promising applications in building, loading, solving, analysis, and optimization. Therefore, the process of studying the construction of finite element model using ANSYS is shown in Fig. 1.

According to Fig. 1, the finite model first selects the elements of the prestressed concrete beam. Secondly, the relevant parameters of the initial finite element modeling are

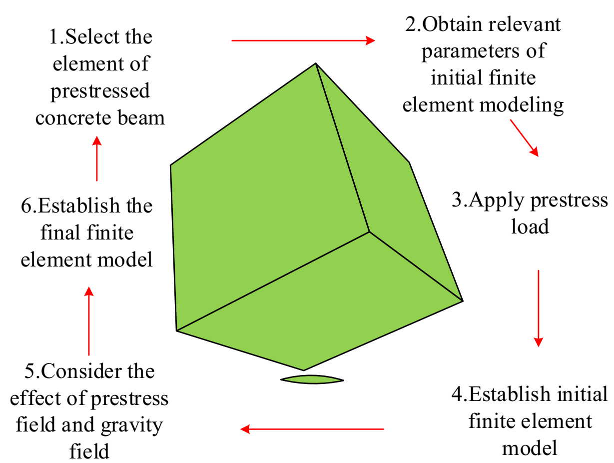

Fig. 1 The specific process of using ANSYS to build an effective meta model

obtained. Then, the initial finite element model is established by applying prestress load. Considering the effect of prestress field and gravity field, the final finite element model is established (For prestressed concrete beam structures, the solid structure will experience upward displacement and deformation under the combined action of prestress and gravity field. Therefore, the theoretical structural entity model established should take into account the influence of pre-stress field and gravity field on the deflection deformation of the beam solid structure when applying loads). The significance of finite element model modification is to adjust and optimize the parameters according to the size of design drawings and material parameters. Combined with the static load test data, it is closer to the measured structural response, so that the optimized finite element model can be used to evaluate its bearing capacity and deformation development. Among them, when applying pre-stressed loads, considering the changes over time, the volume of concrete in pre-stressed concrete shrinks and creeps with the passage of time, causing a certain loss of pre-stress. Therefore, the cooling method is selected to apply prestress, and its expression is shown in Formula (1).

$$T = \frac{F'}{E\alpha A} = \frac{\sigma_{ze}}{E\alpha} \tag{1}$$

In Eq. (1), T denotes the corresponding load prepared for application in the temperature field; F' represents the corresponding prestress applied on the prestressed steel strand; E denotes the modulus of elasticity of the strand; α denotes the coefficient of linear expansion of the strand; A denotes the area of the cross section of the strand; and σ_{ze} denotes the effective prestress value. However, in the practical theoretical application, the response surface method (RSM) is needed to modify the finite model, that is, reasonable experimental methods and parameter significance analysis are used to determine the most influential correlation factor. The response surface equation is fitted to obtain the response surface equation formed by combining important parameters and structural response data. The equation is optimized by combining the relevant experimental data of static and dynamic loads. RSM is a method to select an appropriate experimental design by using the undetermined coefficient method, so as to obtain the combination of multiple experimental data, and thus establish the functional relationship between reaction data and factor parameters (Khalid 2022). The process of RSM is shown in Fig. 2.

From Fig. 2, the RSM process is firstly to establish the numerical computational model; secondly to carry out the corresponding experimental design; then to construct the numerical computational sample and to perform ANOVA with the fitting of the response surface model as a judgment. If the fitted accuracy does not meet the actual demand, the numerical calculation sample is constructed again by adding experiment-related samples and repeating the process. If it is satisfied, the response surface model is output, the objective function is constructed, and the designed parameters are initialized for a second determination. If the initialized parameters do not converge, the design parameters are

Fig. 2 Process of response surface methodology

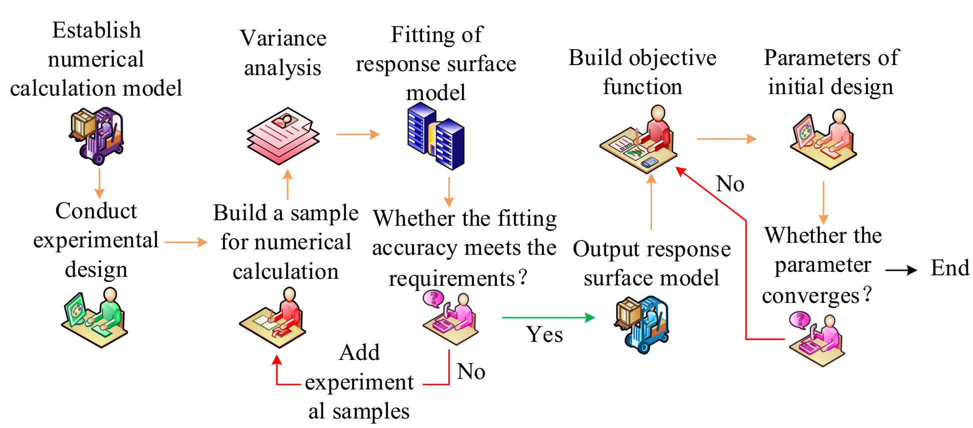

reinitialized, and the cycle is repeated until convergence. Finally, the result value is output.

Study of finite element model modification based on response surface method

In the process of updating the finite element model using the response surface method, assessing the parameter significance has a large proportion. The reason for this is mainly that there are many uncertainties in the initial finite element model, such as boundary conditions, parameter characteristics, etc. Those factors have significant and insignificant effects on the structural response. The effect on structural response such as displacement, deformation, etc. is a significant evaluation process. The influence on the structural response changes over time, so screening out the factors that have a significant influence is a proven measure. Meanwhile, during the actual construction process, the performance of concrete and reinforcement will change somewhat due to the construction environment, labor, and other factors. Therefore, analysis of variance (F-test) must be used for parameter significance screening to determine the significance of each parameter, and make the theoretical model and the structural response in the field have similar results under the same load [24]. It is assumed that the factors present in the engineering design space have multiple levels and that the relevant samples at multiple levels originate from a normal distribution with the same variance as well as the mean. In this case, the variance and the mean are unknown states and the levels are independent of each other. Therefore, the mathematical model expression of one-way ANOVA is shown in Eq. (2).

$$\begin{cases} X_l = \delta_l + \varepsilon_{lw} \\ \varepsilon_{lw} \sim N\left(0, \sigma^2\right) \end{cases} \tag{2}$$

In Eq. (2), X_l denotes the factors in the normal distribution; δ_l denotes the mean; ε_{lw} denotes the level of the sample; $N\left(0, \sigma^2\right)$ denotes the normal distribution; and σ^2 denotes the variance. The expressions of l and w are shown in Eq. (3).

$$\begin{cases} l = 1, 2, \cdots, n \\ w = 1, 2, \cdots, m \end{cases} \tag{3}$$

In Eq. (3), l represents the total number of experiments; w represents the actual number of levels, and its maximum value is o. The purpose of ANOVA is to check whether the means of multiple overall normal distributions are equal, so it is assumed that their overall mean expressions are shown in Eq. (4).

$$\overline{X} = \frac{1}{p} \sum_{w=1}^{o} \sum_{l=1}^{p_w} X_{lw} \tag{4}$$

In Eq. (4), $\overline{X}$ represents the overall mean of the data. Where the expression of p is shown in Eq. (5).

$$p = \sum_{w=1}^{o} p_w \tag{5}$$

In Eq. (5), p_w represents the number of experiments at w levels. the corresponding overall deviation sum of squares expression is introduced as shown in Eq. (6) on the basis of Eq. (4) and is (5).

$$SST = \sum_{W=1}^{o} \sum_{L=1}^{p_w} \left(X_{LW} - \overline{X} \right)^2 \tag{6}$$

In Eq. (6), SST represents the sum of squares of the overall offset. The expression for setting the sample mean at a certain level based on Eq. (6) is shown in Eq. (7).

$$\overline{X}_w = \frac{1}{p} \sum_{l=1}^{p_w} X_{lw} \tag{7}$$

In Eq. (7), $\overline{X}_w$ represents the average value of the sample at level A_w. Sum of Squares of intra group Errors (SSE) and Sum of Squares within the group (SSA) are introduced here. Their expressions and relationships with SST are shown in Eq. (8).

$$\begin{cases} SSE = \sum_{w=1}^{o} \sum_{l=1}^{p_w} \left(X_{lw} - \overline{X} \right)^2 \\ SSA = \sum_{w=1}^{o} \sum_{l=1}^{p_w} \left(\overline{X}_w - \overline{X} \right)^2 \\ SST = SSE + SSA \end{cases} \tag{8}$$

According to Eq. (8), the expression to test the truth of the hypothesis can be given as shown in Eq. (9).

$$\begin{cases} F = \dfrac{SSA/(o-1)}{SSE/(p-o)} \sim F(o-1, p-o) \\ F = \dfrac{SSA/(o-1)}{SSE/(p-o)} \geq F(o-1, p-o) \end{cases} \tag{9}$$

In Eq. (9), F denotes the F-value of the F-test method. Where, the first row is the expression when the hypothesis test is true. The second row is the expression when the hypothesis test is false, when there is a tendency for the F value to be biased. Therefore, the rejection domain of the given significance level α is usually consistent with the state of the hypothesis test being false, taking values of both 0.01 and 0.05. If $F \geq F_{0.01}$, the one-factor significance is high; if $F_{0.05} \leq F \leq F_{0.01}$, the factor is generally significant; if $F < F_{0.05}$, it is not significant. In addition, the construction of the objective function also exerts an influence on the response surface model. The study chose the weighting factor by comparison to assign the data of displacement-deformation and the related stress–strain, and its expression is shown in Eq. (10).

$$f_s(x) = \sum_{1}^{k} r_l \left(1 - {\mu_{aw}}/{\mu_{tw}}\right) \tag{10}$$

In Eq. (10), k represents the upper limit of the design variable. $f_s(x)$ denotes the objective function constructed on the basis of the static test deflection. r_l denotes the weighting factor of the static displacement. μ_{aw} denotes the theoretical calculated value of the deflection, and μ_{tw} denotes the actual measured value of the deflection. Therefore, based on the finite element calculation, it can be transformed and its expression is shown in Eq. (11).

$$f_s = r_1\left(1 - {pd_1}/{ps_1}\right)^2 + r_2\left(1 - {pd_2}/{ps_2}\right)^2 + r_3\left(1 - {pd_3}/{ps_3}\right)^2 + r_4\left(1 - {pd_4}/{ps_4}\right)^2 + r_5\left(1 - {pd_5}/{ps_5}\right)^2 + r_6\left(1 - {pd_6}/{ps_6}\right)^2 + r_7\left(1 - {pd_7}/{ps_7}\right)^2 \tag{11}$$

In Eq. (11), pd represents the finite element calculated value of lateral deflection; ps represents the finite element calculated value of vertical deflection. At this point, the response surface model can be evaluated using a reasonable experimental design to make a judgment. Before that, the complex correlation coefficient needs to be introduced for evaluation, and its expression is shown in Eq. (12).

$$R = \sqrt{\frac{SSR}{SST}} \tag{12}$$

In Eq. (12), R denotes the complex correlation coefficient; SSR represents the sum of the corresponding squares of the regression; SST represents the sum of squares of the population. The complex correlation coefficient measures the accuracy of regression analysis by the ratio of the total square sum of quadratic regression SSR to SST. The nearer its value is to 1, the better the regression accuracy is. Finally, the posterior optimization for the revised response surface model, which is essentially the optimization of the constructed objective function, is expressed as shown in Eq. (13).

$$\begin{cases} \min f(x) \\ h_l(x) = 0 \\ g_l(x) \geq 0 \end{cases} \tag{13}$$

In Eq. (13), $f(x)$ is the correlation function of the target; $h_l(x) = 0$ denotes the relevant constraints of the equation; $g_l(x) \geq 0$ denotes the relevant constraints of the inequality. The expressions of the objective function and the constraint function are shown in Eq. (14) and Eq. (15).

$$\min f(x) = \min \left[Fobj_s(x)\right] \tag{14}$$

In Eq. (14), $\min f(x)$ denotes the minimum value of the objective function and x denotes the function independent variable.

$$\begin{cases} g_l(x) = \begin{cases} R_p - r_u \\ r_1 - R_p \end{cases} \\ Ax - b \leq 0 \end{cases} \tag{15}$$

In Eq. (15), R_p denotes the response surface equation associated with the static deflection; r_u denotes the upper bound of the static response deflection; r_1 denotes the lower bound of the static response deflection; A denotes the coefficient matrix of the linear constraint at the design variable, and b denotes the constraint vector representing the linear constraint at the design variable. On this basis, the finite element model correction of the response surface method is shown in Fig. 3.

From Fig. 3, the correction of the finite element model using the response surface method contains the relationships between the design-related parameters, the variables of the state, and the objective function; the response surface fitting method using the Box-Behnken experimental design; the screening of the significance of the parameters; the fitting of the response surface and the accuracy rating of the response surface equation. Among them, the three variable relationships such as design parameters contain in turn design and state variables. In addition, the study introduces Genetic Algorithm (GA), which is an evolutionary algorithm that mimics the "survival of the fittest" in the biological world, in order to find the optimal solution for the modified model. It is characterized by the ability to directly encode, replicate,

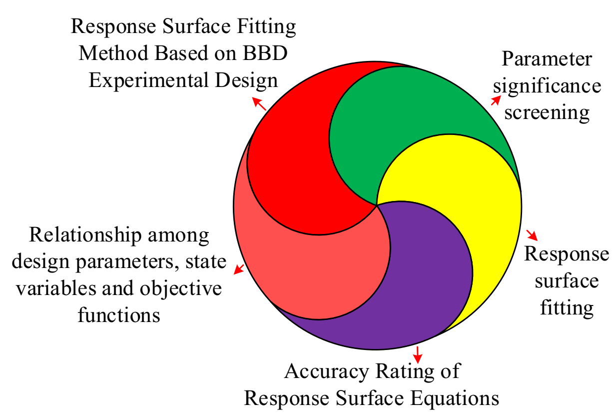

Fig. 3 Using response surface method to modify the specific contents of the finite element model

crossover, and mutate targets, and is not affected by the optimization direction and features, so that the population optimization search space can be automatically extracted and selected, and the optimization direction and method can be adjusted at will, which has a better global optimization performance (Feng et al. 2022).

Analysis of the effect of response surface model in the application of concrete beam structure damage identification

To verify the application effect of finite element model modified by response surface method in damage identification of concrete beam structure, the experimental analysis is carried out. Before the experiments, the corresponding parameter values of state variables and damage settings are set, which are shown in Table 1.

In Table 1, R1-R7 are the different static responses. As can be seen from the table, the settings of the experimentally relevant state variables obeyed the upper and lower limits of 10% as a limit, and the overall values were maintained between − 9 and − 2. The data for the degree of damage are set between 5 and 32%, the initial elastic model is set to 50 GPA, the initial load is applied to 46,875 N, and the initial temperature of the prestress is set at 293 °C. In addition, the finite element model of the elastic modulus to be corrected is set up with relevant data from no damage to 30% damage, for a total of three levels with values ranging from 35 values to 50. Based on this, the study first compares the deflection and strain at the key point location with the actual measured points after the model is corrected, as well as comparing the initial and corrected parameters of the finite element model. The corresponding results are shown in Table 2.

In Table 2, EC denotes the modulus of elasticity of concrete. ES is the elastic modulus of prestressed steel rope itself. DC denotes the density of concrete, and T denotes the loading temperature of the prestress. From the table, it can be seen that the deflection in the span and mid-span section and the strain value in the mid-span section of the concrete beam structure are within 5% under static load, and only the two nodes close to the ends of the supports are around 10%, but they all meet the engineering tolerance error, which shows that the application of the response surface method in the finite element model correction is successful. It also shows that the modified finite element model can effectively evaluate and predict the damage of the structure. Therefore, the study analyzed the significance of the parameters after the response based on the content of the finite element model correction of the response surface method, and the results are shown in Fig. 4.

In Fig. 4, the influence factor combinations selected in the study are all significant influence factor combinations, and their numerical results are the F values of the response results, which are obtained after the F variance test. In addition, 1–8 represent 8 parameter combinations, namely concrete modulus, concrete density, concrete Poisson's ratio, steel strand modulus, steel strand Poisson's ratio, steel strand applied temperature, and the square of the first three parameter values. From Fig. 4 that according to different combinations of significant influencing factors, R1-R7's own deflection changes have high sensitivity in the loss settings related to elastic modulus. Based on the parameter significance results, the research continued to analyze the accuracy of its response surface equation, and the results are shown in Fig. 5.

In Fig. 5, the accuracy of the response surface equations is evaluated by the complex correlation coefficient. From the figure that the evaluation coefficients of the seven static responses are all higher than 0.99, which is very close to

Table 1 Parameter setting contents of relevant parts of the experiment

		R1	R2	R3	R4	R5	R6	R7
State variable	Experimental data (mm)	− 2.87	− 4.52	− 6.79	− 7.92	− 6.99	− 4.88	− 2.90
	Upper limit (mm)	− 3.00	− 4.75	− 7.12	− 8.32	− 7.34	− 5.12	− 3.04
	Lower limit (mm)	− 2.72	− 4.29	− 6.45	− 7.52	− 6.64	− 4.63	− 2.75
Elastic modulus damage	Damage setting degree (%)	10	20	30	20	15	5	
	Elastic modulus EC (GPA)	40.4	35.9	31.4	31.4	35.9	40.4	
Damage state		Level 1			Level 2		Level 3	
	L/8 lower left	35			40		50	
	L/8 lower left-3.75 M lower part	35			40		50	
	3.75 M-Lower part of midspan section	35			40		50	
	Upper part of midspan section-4.25 M upper part	35			40		50	
	4.25 M-7L/8 upper part	35			40		50	
	7L/8 left upper part—upper part of support position	35			40		50	

Table 2 Comparison of key point position parameters before and after model modification

Comparison of data related to key positions after correction

Working condition	Size of prestressing force					Load			
	$0.35F_{yk}$					56.3KN·M			
Measuring point position	L/8	2L/8	3L/8	4L/8	5L/8	6L/8	7L/8	Mid span upper edge	Mid span bottom plate
Measured value	– 0.20 mm	– 0.51 mm	– 0.80 mm	– 0.93 mm	– 0.85 mm	– 0.56 mm	– 0.21 mm	– 33.00 με	57.00 με
Before amendment	– 0.25 mm	– 0.56 mm	– 0.86 mm	– 1.00 mm	– 0.86 mm	– 0.56 mm	– 0.25 mm	– 40.90 με	68.20 με
After correction	– 0.22 mm	– 0.51 mm	– 0.83 mm	– 0.94 mm	– 0.86 mm	– 0.56 mm	– 0.23 mm	– 35.27 με	60.60 με
Deviation before correction (%)	23.79	13.99	8.50	7.30	2.34	1.69	18.09	24.00	19.20
Deviation after correction（%）	9.49	3.99	3.69	1.00	2.29	1.69	9.00	6.90	5.20

Finite element model parameters

	EC	DC	ES	T
Initial parameters	34.50 0GPA	2500 kg/m³	195.00	312 °C
Response surface correction	38.01GPA	2580 kg/m³	195.05	293 °C
Ratio	1.10	1.03	1.00	0.94 °C

Comparison of data related to key positions after correction

Working condition	Prestress size					Load			
	$0.35F_{yk}$					56.3KN-M			
Measuring point position	L/8	2L/8	3L/8	4L/8	5L/8	6L/8	7L/8	Upper mid-span edge	Midspan baseplate
Measured value	– 0.20 mm	– 0.51 mm	– 0.80 mm	– 0.93 mm	– 0.85 mm	– 0.56 mm	– 0.21 mm	– 33με	57με
Before amendment	– 0.25 mm	– 0.56 mm	– 0.86 mm	– 1.00 mm	– 0.86 mm	– 0.56 mm	– 0.25 mm	– 40.9με	68.2με
After correction	– 0.22 mm	– 0.51 mm	– 0.83 mm	– 0.94 mm	– 0.86 mm	– 0.56 mm	– 0.23 mm	– 35.27με	60.60με
Deviation before correction (%)	23.79	13.99	8.50	7.30	2.34	1.69	18.09	24.00	19.20
Deviation after correction (%)	9.49	3.99	3.69	1.00	2.29	1.69	9.00	6.90	5.20

Finite element model parameters

	EC	DC	ES	T
Initial parameters	34.50 0GPA	2500 kg/m³	195.00	312 °C
Response surface correction	38.01GPA	2580 kg/m³	195.05	293 °C
Ratio	1.10	1.03	1.00	0.94 °C

1, indicating that the fitting accuracy of their response surface equations is high. Therefore, the corresponding surface equations are used to modify the finite element model, and the modified model has high accuracy in the structural identification of concrete beams. Meanwhile, based on the results in Fig. 4 and Fig. 5, it can be used to realize the optimal calculation of the finite element model modification by response surface method, and then identify the damage of concrete beam structure. For the study, a certain concrete beam of a project, calibrated as a $1^{\#}$ beam, was selected in practice. Before its structural damage identification, to determine the effectiveness of the correction of the functional algorithm model and the GA model, the study first compared the two for analysis, and the results are shown in Fig. 6.

From Fig. 6 that most of the revised values of the two algorithm models are higher than the initial parameters, and most of the ratios are greater than 1.0. Only the T ratio is lower than 1.0. The genetic algorithm is 0.929, and the functional algorithm is 0.939. In addition, the revised values of the two algorithms are roughly the same, with only 0–2 differences. The results show that the two algorithms can be used to evaluate the bearing capacity of concrete beam structures, and the response surface method is effective for finite element model updating. On this basis, the comparison

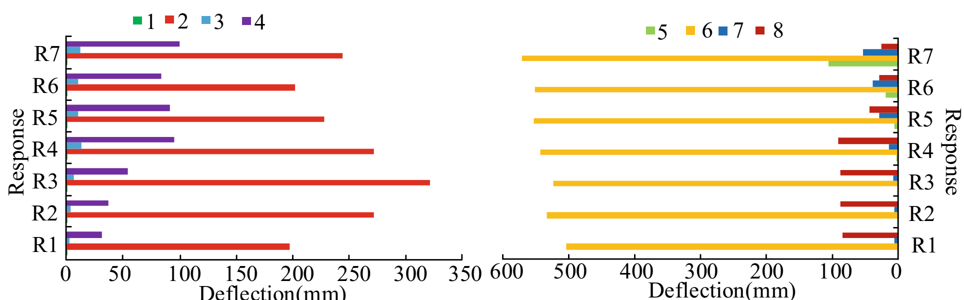

Fig. 4 Parameter significance results after response

(a) Parameter significance results of the first four combinations (b) Parameter significance results of the last four combinations

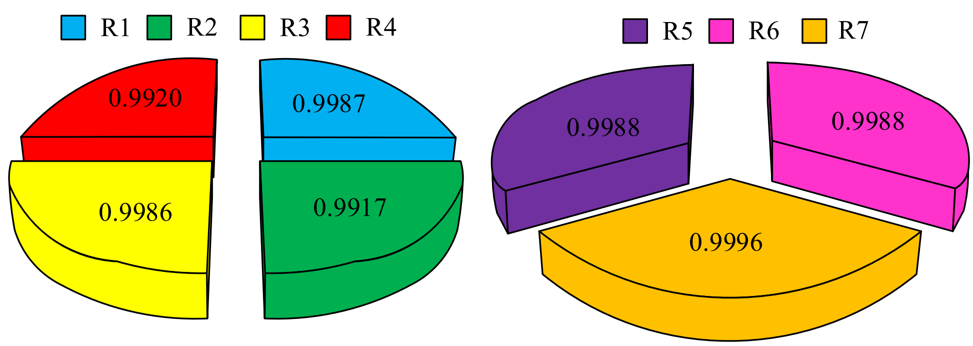

Fig. 5 Accuracy evaluation results of response surface equation

(a) Accuracy evaluation results of static response R1-R4 (b) Accuracy evaluation results of static response R5-R7

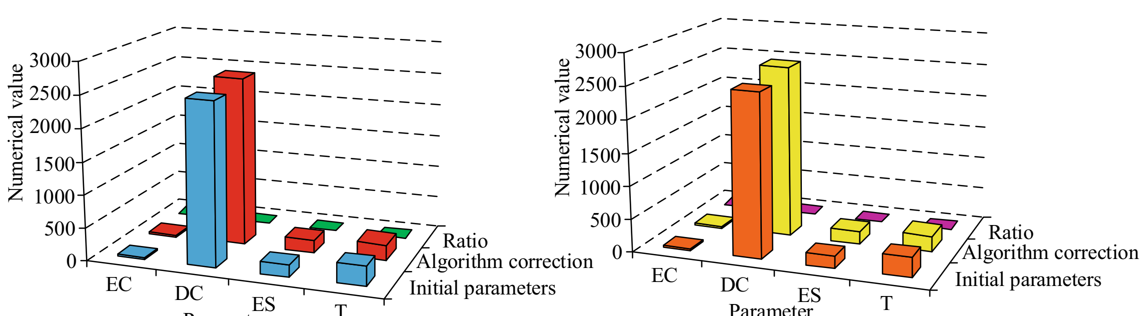

(a) GA model correction results (b) Correction results of function algorithm model

Fig. 6 Correction results of functional algorithm model and GA model between the response surface function optimization results and the response surface GA optimization results, and the measured results is analyzed. The results are shown in Fig. 7.

In Fig. 7, 1# beams are optimally solved on the finite element response surface and compared with the deflection of the beam after three loadings. Meanwhile, the horizontal axes 1–7 represent the seven different critical point locations in Table 2. From the figure, the deflection contrast values at each critical point are less than 10%, with the lowest being 1.1%. The results of function optimization and genetic algorithm optimization basically fit with the actual results and show high accuracy. Therefore, the results obtained by applying them to the actual damage condition identification are shown in Fig. 8.

In Fig. 8, the horizontal axes 1–6 indicate the parameters of the design, i.e., the elastic modes of the six zones. A and B indicate the damage value and the optimized value of the initial value setting, respectively. From the figure, the force damage of the concrete beam is mainly concentrated in the area of concentrated load in the span, followed by the combined moment-shear zone, which is consistent with the stress response deformation characteristics of the actual concrete beam. It shows that the finite element model modified by response surface method is effective in damage identification.

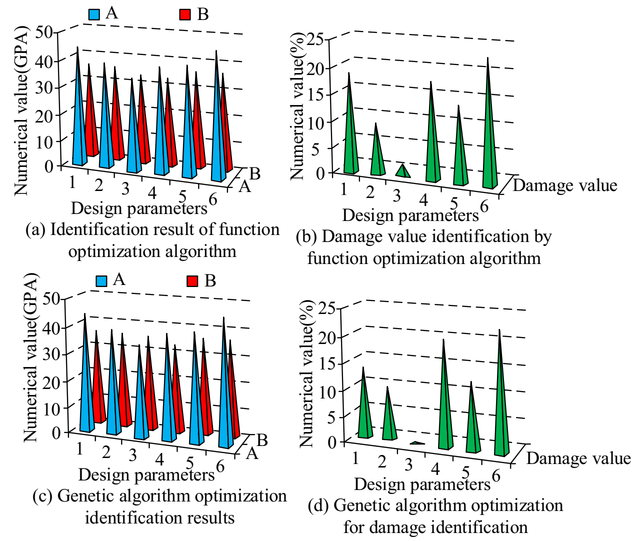

Fig. 8 Damage identification results of two algorithm models

Fig. 7 Comparison between the optimized results of the two algorithms and the measured results

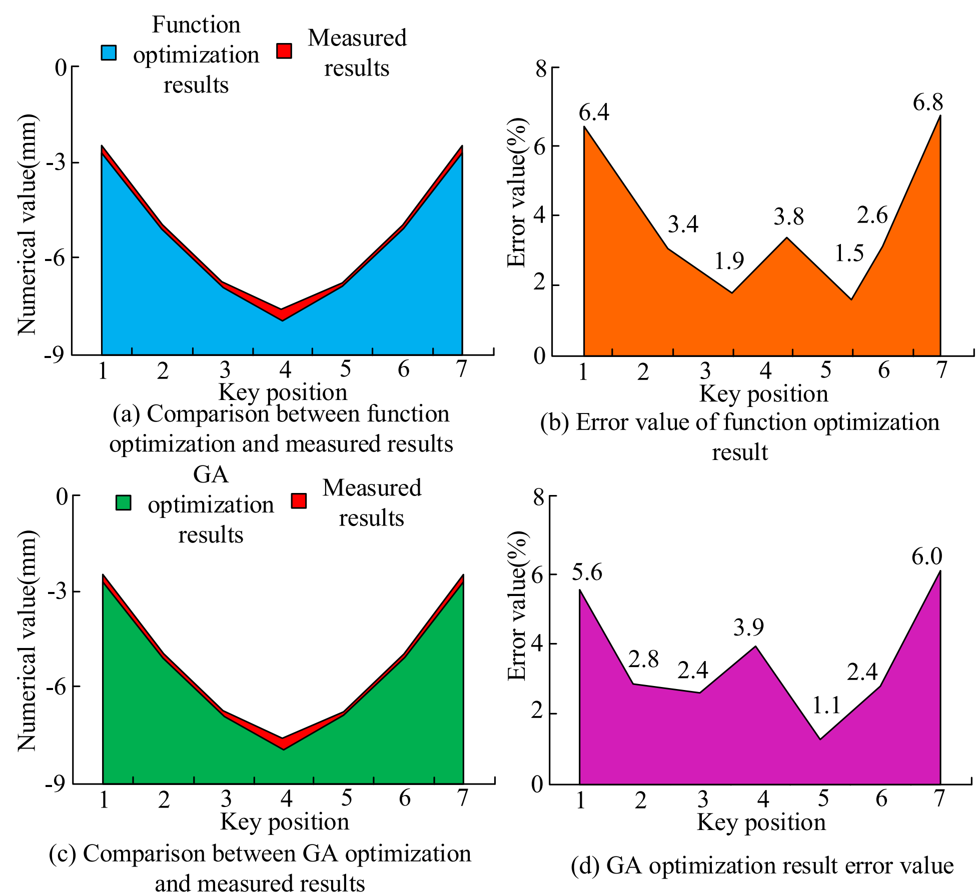

Conclusion

To realize the effective identification of concrete beam structure damage, response surface method is used to modify the finite element model, and GA algorithm is introduced to optimize it. Its effectiveness is verified in actual experiments. The experimental results show that the deformation and strain values of the midspan and its section of the concrete beam under static load are within 5%, and only two positions near the supporting end are within 10%. The deflection changes of different static responses are within the damage setting range of concrete structures, and have high sensitivity. The accuracy evaluation value of response surface equation for different static responses is higher than 0.99, which indicates that the fitting accuracy of the modified finite element model is higher. After using the two optimization algorithms, the fitting curves of the predicted values and the actual measured values are basically consistent, and the offset contrast values are less than 10%. In the actual damage identification of concrete beam structure, the characteristics of stress response and deformation are consistent with those of the actual concrete beam, showing high accuracy. In a word, the response surface modified finite element model can effectively judge the bearing capacity of concrete beam structure, and under the optimization of GA and other algorithms, the damage identification accuracy of the model is effectively improved. However, the modification of the finite element model established in the study is relatively simple, and it cannot be verified that the response surface model modification under static loading has a good reflection on the dynamic response characteristics of the concrete beam structure, which are the limitations and needs further analysis in the future.

Declarations

Conflict of interest The authors have no-relevant financial or non-financial interests to disclose.

References

Cui, M., Wu, G., Dang, J., Chen, Z., Zhou, M.: Deep learning-based condition assessment for bridge elastomeric bearings. J. Civ. Struct. Heal. Monit. **12**(2), 245–261 (2022)

De Risi, R.: A computational framework for finite element modeling of traveling loads on bridges in dynamic regime. Comput.-Aided. Civ. Infrastruct. Eng. **37**(4), 470–484 (2022)

Deng, Y., Zhang, Y., Luo, X., Lytton, R.L.: Development of equivalent stationary dynamic loads for moving vehicular loads using artificial intelligence-based finite element model updating. Eng. Comput. **38**(4), 2955–2974 (2022)

Feng, Y., Lan, C., Briseghella, B., et al.: Cable optimization of a cable-stayed bridge based on genetic algorithms and the influence matrix method. Eng. Optim. **54**(1), 20–39 (2022)

Jawdhari, A., Peiris, A., Harik, I.: Load rating of bridge-size reinforced concrete arch culverts. Struct. Infrastruct. Eng. **18**(3), 362–375 (2022)

Khalid, U.: Optimization of COVID-19 face mask waste fibers and silica fume as a balanced mechanical ameliorator of fat clay using response surface methodology. Environ. Sci. Pollut. Res **29**(12), 17001–17016 (2022)

Li, X., Fu, X., Gu, L.: Research on bridge structural health assessment based on finite element analysis. Tehnički Vjesnik **27**(1), 96–105 (2020)

Lin, S.T.K., Lu, Y., Alamdari, M.M., Khoa, N.L.D.: Neural network based numerical model updating and verification for a short span concrete culvert bridge by incorporating Monte Carlo simulations. Struct. Eng. Mech. **81**(3), 293–303 (2022)

Ma, F., Li, H., Hou, S., Kang, X., Wu, G.: Defect investigation and replacement implementation of bearings for long-span continuous box girder bridges under operating high-speed railway networks: a case study. Struct. Infrastruct. Eng. **18**(5), 678–693 (2022)

Manoj, S., Choudhury, D., Alzaylaie, M.: Value engineering using load-cell test data of barrette foundations–La Maison, Dubai. Proc. Inst. Civ. Eng-Geotech. Eng. **175**(3), 340–352 (2022)

Naranjo-Pérez, J., Jiménez-Alonso, J.F., Pavic, A., Sáez, A.: Finite-element-model updating of civil engineering structures using a hybrid UKF-HS algorithm. Struct. Infrastruct. Eng. **17**(5), 620–637 (2021)

Skokandić, D., Mandić, I.A.: Value of additional traffic data in the context of bridge service-life management. Struct. Infrastruct. Eng. **18**(4), 456–475 (2022)

Song, S.T., Hu, T.F., Chiou, D.J.: Influence of riverbed scour on the performance of bridges subjected to lateral seismic loads. J. Earthquake Eng. **26**(5), 2251–2282 (2022)

Souza Hoffman, I., Manica Lazzari, B., Campos, A., et al.: Finite element numerical simulation of a cable-stayed bridge construction through the progressive cantilever method. Struct. Concr. **23**(2), 632–651 (2022)

Svendsen, B.T., Petersen, Ø.W., Frøseth, G.T., Rønnquist, A.: Improved finite element model updating of a full-scale steel bridge using sensitivity analysis. Struct. Infrastruct. Eng. **19**(3), 315–331 (2022)

Tran-Ngoc, H., Khatir, S., Le-Xuan, T., De Roeck, G., Bui-Tien, T., Abdel, W.M.: Finite element model updating of a multispan bridge with a hybrid metaheuristic search algorithm using experimental data from wireless triaxial sensors. Eng. Comput. **38**(3), 1865–1883 (2022)

Wang, H., Liu, J., Wen, G.: An efficient multi-resolution topology optimization scheme for stiffness maximization and stress minimization. Eng. Optim. **54**(1), 40–60 (2022)

Wei, B., Wang, W.H., Wang, P., Yang, T.H., Jiang, L.Z.: Seismic responses of a high-speed railway (HSR) bridge and track simulation under longitudinal earthquakes. J. Earthquake Eng. **26**(9), 4449–4470 (2022)

Wu, D., Liu, L.: Study on iterative modification method of parameters in the health monitoring of large-span continuous rigid frame bridges. J. Inst. Eng. (India) Ser. A **103**(1), 271–281 (2022)

Yu, J., Jiang, L., Zhou, W., Liu, X., Lai, Z., Feng, Y.: Study on the dynamic response correction factor of a coupled high-speed train–track–bridge system under near-fault earthquakes. Mech. Based Des. Struct. Mach. **50**(9), 3303–3321 (2022)

Zaghian, S., Martín-Pérez, B., Almansour, H.: Nonlinear finite element modeling of the impact of reinforcement corrosion on bridge piers under concentric loads. Struct. Concr. **23**(1), 138–153 (2022)

Zhang, Z., Sun, C.: Structural damage identification via physics-guided machine learning: a methodology integrating pattern recognition with finite element model updating. Struct. Health Monit. **20**(4), 1675–1688 (2021)

Zhu, L., Wang, Y., Zhou, G., Han, B.: Structural health monitoring on a steel-concrete composite continuous bridge during construction and vehicle load tests. Mech. Adv. Mater. Struct. **29**(10), 1370–1385 (2022)